Selectively electron transparent microstamping toward concurrent digital image correlation and high resolution EBSD analysis

T.J. Ruggles[a,*], G.F. Bomarito[b], A.H. Cannon[c,d], J.D. Hochhalter[b]

[a]*National Institute of Aerospace, Hampton, VA, USA*
[b]*National Aeronautics and Space Administration, Langley Research Center, Hampton, VA, USA*
[c]*1900 Engineering, LLC, Clemson, SC, USA*
[d]*Clemson University, Department of Chemical and Biomolecular Engineering, Clemson, SC, USA*

Abstract

High resolution digital image correlation (HRDIC) and high resolution electron backscatter diffraction (HREBSD) provide valuable and complementary data concerning local deformation at the microscale. However, standard surface preparation techniques are mutually exclusive, which makes combining these techniques *in situ* impossible. This paper introduces a new method of applying surface patterning for HRDIC, namely a urethane rubber microstamp, that provides a pattern with enough contrast for HRDIC at low accelerating voltages, but is still virtually transparent at the higher voltages necessary for HREBSD and conventional electron backscatter diffraction (EBSD) analysis. Furthermore, microstamping is inexpensive and repeatable, and is more amenable to application of patterns to complex surface geometries and larger surface areas than other patterning techniques.

Keywords: High resolution EBSD, EBSD, digital image correlation, lithography, microstamping

1. Introduction

Recent advances in two scanning electron microscopy (SEM) characterization techniques high resolution electron backscatter diffraction (HREBSD) and high resolution digital image correlation (HRDIC), allow for microscale resolution of the total local deformation (HRDIC) (Yan et al., 2015; Gupta et al., 2014), and the local elastic strain and geometrically necessary dislocation (GND) content (HREBSD) (Jiang et al., 2016; Ruggles et al., 2016b) of crystalline materials. Data from these microscopy techniques can be used to validate and develop high fidelity plasticity models (Lim et al., 2014; Zhang et al., 2014; Lim et al., 2015; Dingreville et al., 2016). The information from HRDIC (total strain) and HREBSD (stress and GND density) is complementary, together providing a decomposition of the elastic and plastic behavior of a crystalline material at the microscale, which offers extended insight into model development. However, these characterization techniques have been mutually exclusive on the same surface at the same length scale, given the current state of sample preparation necessary for each technique. A sample well polished for EBSD does not contain

sufficient features for HRDIC measurement, and applied patterns for HRDIC disrupt EBSD diffraction. This has limited the use of EBSD on HRDIC patterned surfaces to initial microstructural characterization, sampling between speckles of the pattern at a higher length scale, and *post mortem* analysis. This paper introduces a new method of HRDIC pattern application, microstamping, that leaves a pattern thin enough to be mostly invisible to EBSD at high accelerating voltages, but still capable of providing enough contrast for HRDIC. This technique allows for the simultaneous collection of HREBSD and HRDIC data *in situ*.

There are a number of established methods of patterning the sample for microscale HRDIC, which have variable compatibility with EBSD techniques. Some patterning techniques degrade EBSD pattern quality but are non-damaging to the surface and removable, allowing for *post mortem* EBSD analysis. Nanoparticle decoration and lithography are two such methods (Kammers & Daly, 2011). It should be noted that EBSD patterns sometimes can be collected despite these patterning techniques, most notably colloidal silica nanoparticles because they are small, amorphous and have a low effective atomic mass (Yan et al., 2015). However, the EBSD pattern quality degrades, making this method potentially problematic for

HREBSD techniques, which require a greater precision than commercially available indexing software. Etching (Ruggles et al., 2016a) and focused ion beam (FIB) patterning (Choi et al., 2014) are also available methods of applying a HRDIC pattern, but these methods are destructive and completely preclude EBSD methods.

This paper proposes a residual layer urethane rubber microstamping as a method for concurrent HREBSD and HRDIC because of its selective transparency to electrons of different energy. A low atomic number, amorphous material is transferred such that it is thin enough to be effectively transparent to the higher energy electrons used for EBSD (typically 20-30 keV), but thick enough to give sufficient contrast for HRDIC at low accelerating voltages (5 keV for this study). In this study, a selectively electron transparent microstamp with a 1 micron speckle size is applied to an aluminum oligocrystal, and its effect on HREBSD techniques and its compatibility with HRDIC are assessed.

2. Methods

Flexible microstamps are fabricated by first creating a rigid master mold and then applying a polymer using a vacuum casting process. Standard methods for photolithography work well for fabricating these molds quickly when the speckle sizes are greater than 1 micron. For sub-micron speckle sizes, the molds should be fabricated using e-beam lithography (EBL) or FIB machining to achieve sufficient resolution in the speckle edges. It has been observed that a 500 nm feature depth is ideal for microstamping. The stamp mold used in this study is 1 × 1 mm with a speckle size of 1 micron fabricated with photolithography. Rather than a random pattern, a pattern was optimized to minimize correlation error consistent with Bomarito et al. (2017).

Once the mold is fabricated, many stamps can be replicated from it inexpensively. For the stamp, a castable elastomer is selected which must be soft and flexible to gently peel away from the master and be useful for pattern reproduction on curved substrates while having sufficient toughness to avoid tearing at the corners of the micro features of the stamp. The material is vacuum cast to the master, expelling all entrapped gas and allowing the material to flow into the sub-micron features of the mold and then polymerized. Selection of the specific elastomer largely depends on the desired method of application.

There are three different methods developed so far to use the stamp to apply a pattern once it is fabricated. The first is displacement stamping, where an ink, typically a

lithography resist, is spin-coated onto the sample and then a silicone rubber stamp is applied to the ink layer and heat is applied to cure the ink (Cannon et al., 2015). The second method is transfer stamping, where ink is applied into the grooves of the stamp and then transferred to the specimen by applying heat and pressure (Cannon et al., 2016; Mello et al., 2016). Transfer stamping works best with traditional inks, such as a vacuum stable dye suspended in alcohol, which is equally compatible with optical and electron microscopy due to its opacity. In contrast, typical lithography resists are largely transparent to optical light. Urethane rubber is used for the stamp material because of its wettability with a variety of inks. A major advantage of the transfer method is that much of the specimen surface remains uncovered by the ink, such that microscopic observations of a relatively pristine surface can be made, even after pattern application. However, a thin residual layer of urethane rubber is deposited to the surface of the material between speckles of the pattern where the stamp itself was in contact with the specimen, which has minimal effect on the collection of EBSD and energy dispersive X-ray spectroscopy (EDS) data.

This thin residual layer of rubber in between ink speckles in transfer stamping led to the development of the third method of transferring a pattern from a microstamp to a specimen: residual layer microstamping. For this method, no ink is applied to the stamp. Instead, heat and pressure are used to melt a thin layer of urethane from the stamp and transfer it to the specimen. The resulting residual layer pattern is thin, on the order of 10 nm (determined via contact profilometry), with the space between speckles left completely untouched. Furthermore, the pattern is thin enough to have a negligible effect on backscatter electrons at high accelerating voltages (20 keV), but still thick enough to be readily imaged via secondary electron imaging at lower accelerating voltages (5 keV). This selective transparency is demonstrated in Figure 1. The suitability of urethane stamp patterns for both HREBSD and HRDIC is further quantified in Section 3.

3. Results

The material selected for this study was an oligocrystal of a binary alloy of aluminum and copper (4 wt.%), the same material used in Gupta et al. (2014). The sample was polished mechanically before a final electropolish. A 200 x 200 micron EBSD map of an area was collected with a step size of 5 microns at 20 keV before and after microstamping using AZtecHKL[TM] software using near identical parameters. The band contrast (a pattern qual-
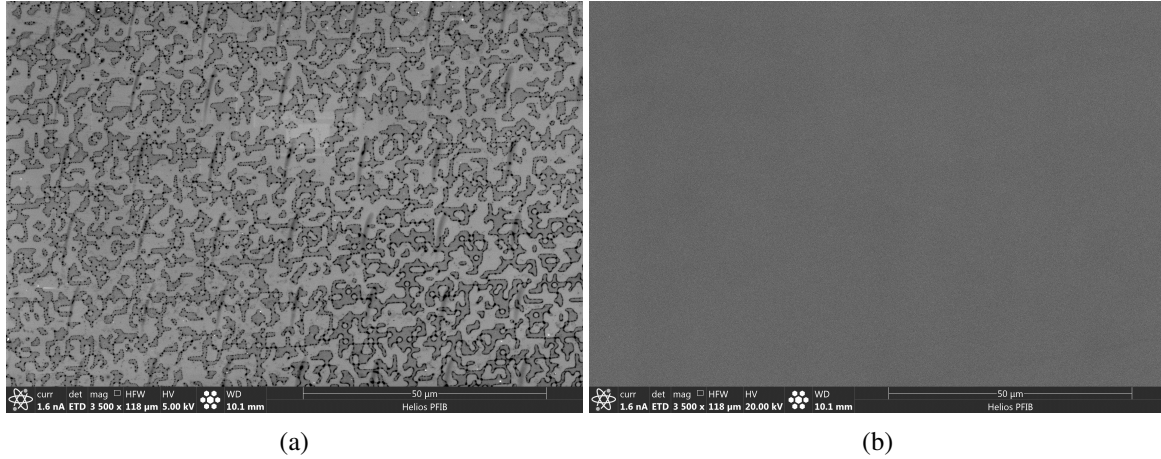
Figure 1: A section of a urethane residual layer stamp applied to an aluminum oligocrystal imaged at 5 keV using secondary electron imaging (a) and at 20 keV using backscatter electrons (b).
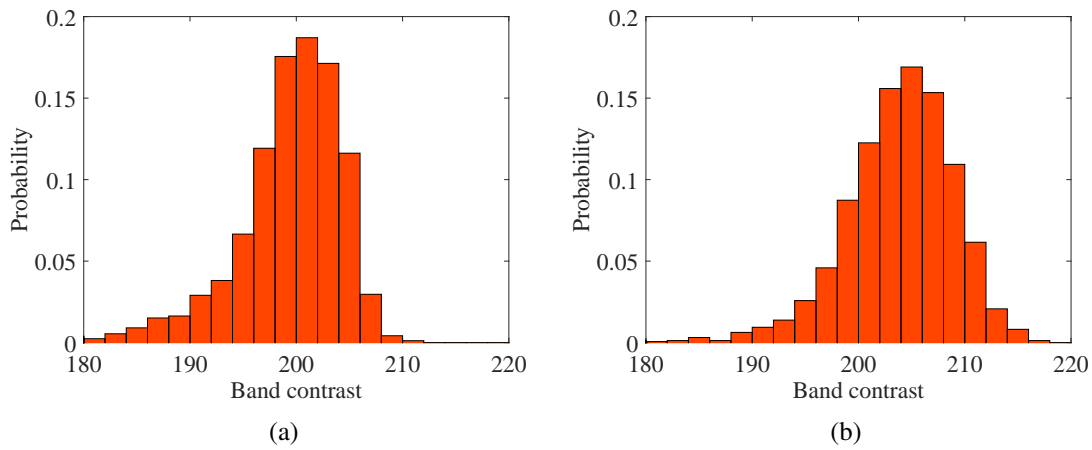

Figure 2: Histograms of the band contrast of a region of an AlCu oligocrystal before (a) and after (b) application of a urethane rubber microstamp.

ity metric) was selected as a metric for the degradation of the quality of the EBSD patterns collected. More familiar metrics, such as fit and confidence index, are more appropriate for conventional EBSD indexing, whereas pattern quality metrics like band contrast better capture the loss of fine detail in a pattern critical for HREBSD measurements (Wilkinson & Britton, 2012). A histogram of the band contrast in the region before (a) and after (b) microstamping is shown in Figure 2. The mean band contrast before and after microstamping actually increased by 5 points, probably due to subtle variations in the operating conditions of the microscope. This negligible difference suggests that the quality of the EBSD patterns is not strongly affected by the application of the urethane HRDIC pattern.

To evaluate the transparency of the pattern to HREBSD techniques, a 50 × 50 micron region of a single large grain was scanned for HREBSD with a step size of 250 nm and binning the patterns 2 × 2. The diffraction patterns were post-processed using OpenXY to calculate strain relative to an arbitrary reference point (Brigham Young University, 2016). Because the oligocrystal from this study was formed in a Bridgman furnace, it may be considered heavily annealed and relatively strain free. Thus, measured strain can be considered erroneous. This strain is plotted in Figure 3. The median value of the norm of this measured strain is 319 microstrain, very close to the theoretical strain resolution of HREBSD with a standard diffraction geometry and phosphor screen resolution using 2 × 2 binning (Jiang et al., 2013). This low level of erroneous strain suggests that the applied urethane rubber pattern has little to no effect on the resolution of HREBSD techniques.

The suitability of the stamped pattern for image correlation was evaluated in a Helios™ scanning electron microscope (SEM). Imaging was performed at a 10.1 mm
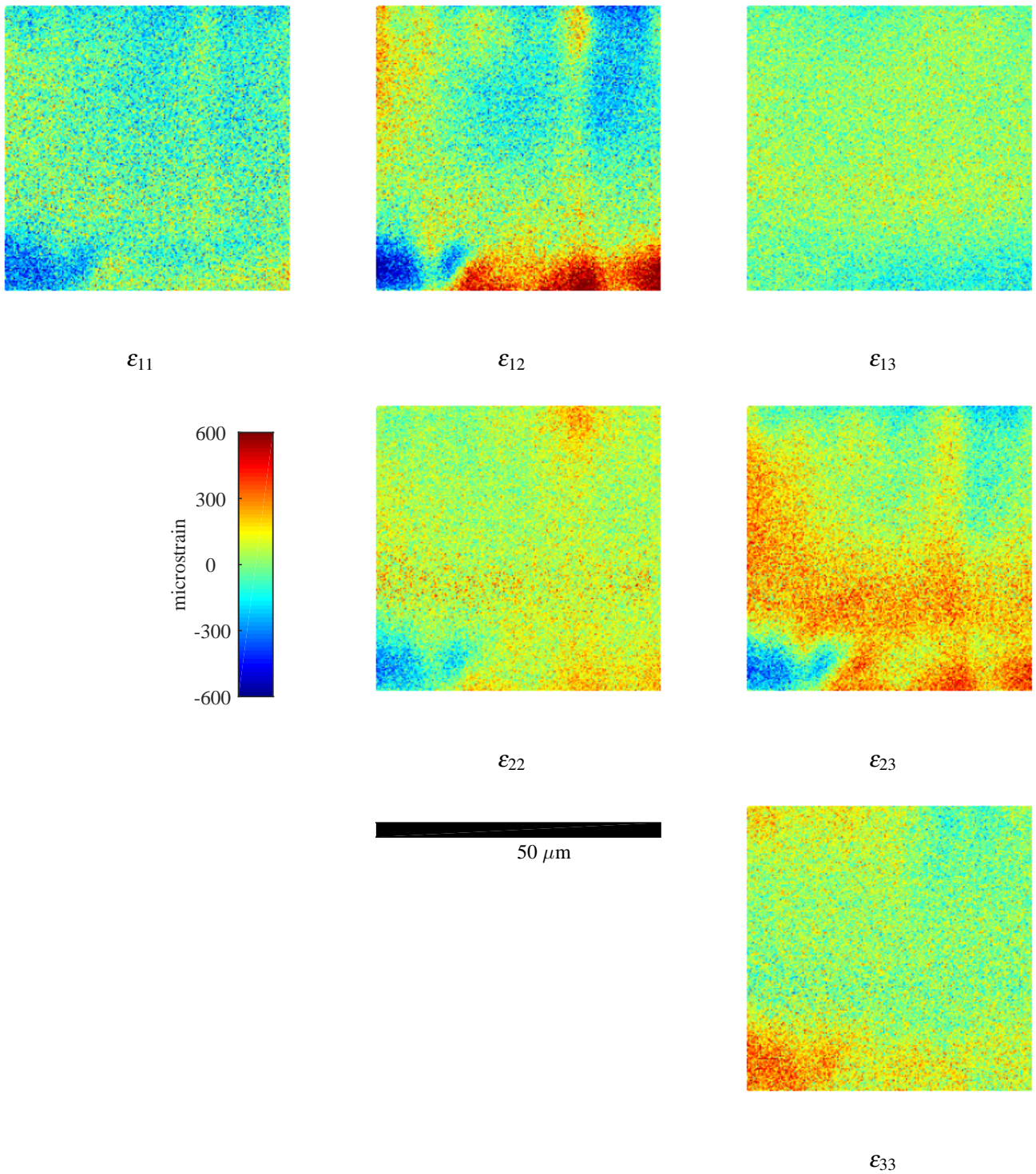
Figure 3: Strain measured over a 50 micron square area of a heavily annealed AlCu oligocrystal with a 250 nm step size. EBSD patterns were binned 2×2. The strain components are given in the reference frame of the sample, where the 3-direction is normal to the surface. The strains measured here are comparable with the theoretical resolution of the method.
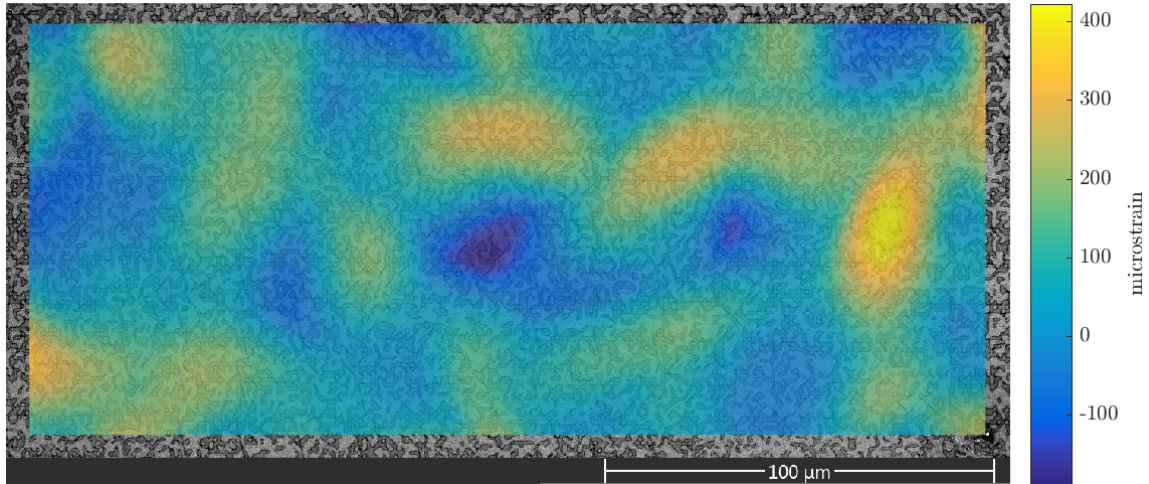
Figure 4: Maximum principal strain erroneously detected via HRDIC after a 10 micron translation in the horizontal direction. The strain contour is overlayed on a micrograph of the urethane rubber correlation pattern.

working distance with an accelerating voltage of 5 keV, a beam current of 1.6 nanoamps and a pixel density of 5.12 pixels per micron. The subset size (an image correlation parameter that approximates the spatial resolution of the technique) was selected to be 55 pixels, or around 10.7 microns. Subset size must be selected to be compatible with the size of the speckles in the pattern (Lecompte et al., 2006), and our subset size was determined using trial and error to achieve the desired strain resolution while maximizing spatial resolution. Image drift calibration for an SEM was performed per the standard operating procedure of the image correlation software employed, VIC2D (Correlated Solutions, 2009). The area was imaged and then translated 10 microns and imaged again. The resulting phantom strains, pictured in Figure 4, had a mean operator 2-norm of 159.1 microstrain, approximately on the order of the strain resolution limit of HREBSD (around 200 microstrain (Wilkinson et al., 2006)). Note that increasing the subset size would improve strain resolution at the expense of spatial resolution, but this subset size was selected to maximize the spatial resolution afforded by the 1 micron speckle size of the stamp, while still maintaining similar strain accuracy to HREBSD.

4. Discussion

This work presents a new method of applying a speckle pattern for high resolution HRDIC in an SEM that does not disrupt EBSD data collection: urethane rubber microstamping. The residual layer of urethane rubber left by this stamping process has sufficient mass for contrast at low accelerating voltages, but has a negligible ef-

fect on the quality of EBSD patterns that can be collected from the underlying surface. This allows for HRDIC and HREBSD, a technique particularly sensitive to the quality of EBSD patterns, to be carried out on the same surface at the same length scale *in situ*. Currently, microstamps have been successfully fabricated with a 1 micron speckle size, which results in a spatial resolution of around 10.7 microns and a strain resolution of around 160 microstrain. The spatial resolution may be improved by refining the speckle size of the stamp. Future work will focus on applying the current 1 micron microstamp to the characterization and modeling of the deformation of oligocrystals as well as developing higher resolution stamps to work at the length scale of engineering materials.

References

BOMARITO, G., HOCHHALTER, J., RUGGLES, T. & CANNON, A. (2017). Increasing accuracy and precision of digital image correlation through pattern optimization, *Optics and Lasers in Engineering* **91**, 73 – 85.

BRIGHAM YOUNG UNIVERSITY (2015–2016). OpenXY, github.com.

CANNON, A.H., HOCHHALTER, J.D., BOMARITO, G.F. & RUGGLES, T.J. (2016). Micro speckle stamping: High contrast, no basecoat, repeatable, well-adhered, *Conference Proceedings of the Society for Experimental Mechanics Series*, International Digital Imaging Correlation Society.

CANNON, A.H., HOCHHALTER, J.D., MELLO, A.W., BOMAR-ITO, G.F. & SANGID, M.D. (2015). Microstamping for improved speckle patterns to enable digital image correlation, *Microscopy and Microanalysis* **21**, 451–452.

CHOI, Y.S., GROEBER, M.A., SHADE, P.A., TURNER, T.J., SCHUREN, J.C., DIMIDUK, D.M., UCHIC, M.D. & ROLLETT, A.D. (2014). Crystal plasticity finite element method simulations for a polycrystalline Ni micro-specimen deformed in tension, *Metallurgical and Materials Transactions A* **45**, 6352–6359.

CORRELATED SOLUTIONS (2009). Vic-2d, *Reference Manual* URL http://www.correlatedsolutions.com.

DINGREVILLE, R., KARNESKY, R.A., PUEL, G. & SCHMITT, J.H. (2016). Review of the synergies between computational modeling and experimental characterization of materials across length scales, *Journal of Materials Science* **51**, 1178–1203.

GUPTA, V.K., WILLARD, S.A., HOCHHALTER, J.D. & SMITH, S.W. (2014). Microstructure-scale in-situ image correlation-based study of grain deformation and crack tip displacements in al–cu alloys, *Materials Performance and Characterization* **4**, 228–253.

JIANG, J., BRITTON, T. & WILKINSON, A. (2013). Measurement of geometrically necessary dislocation density with high resolution electron backscatter diffraction: Effects of detector binning and step size, *Ultramicroscopy* **125**, 1–9.

JIANG, J., ZHANG, T., DUNNE, F.P.E. & BRITTON, T.B. (2016). Deformation compatibility in a single crystalline Ni superalloy, *Proceedings of the Royal Society of London A: Mathematical, Physical and Engineering Sciences* **472**, 1–24.

KAMMERS, A.D. & DALY, S. (2011). Small-scale patterning methods for digital image correlation under scanning electron microscopy, *Measurement Science and Technology* **22**, 125501.

LECOMPTE, D., SMITS, A., BOSSUYT, S., SOL, H., VANTOMME, J., HEMELRIJCK, D.V. & HABRAKEN, A. (2006). Quality assessment of speckle patterns for digital image correlation, *Optics and Lasers in Engineering* **44**, 1132 – 1145.

LIM, H., CARROLL, J.D., BATTAILE, C.C., BOYCE, B.L. & WEINBERGER, C.R. (2015). Quantitative comparison between experimental measurements and CP-FEM predictions of plastic deformation in a tantalum oligocrystal, *International Journal of Mechanical Sciences* **92**, 98 – 108.

LIM, H., SUBEDI, S., FULLWOOD, D., ADAMS, B. & WAGONER, R. (2014). A practical meso-scale polycrystal model to predict dislocation densities and the Hall-Petch effect, *Materials Transactions* **55**, 35–38.

MELLO, A.W., NICOLAS, A., LEBENSOHN, R.A. & SANGID, M.D. (2016). Effect of microstructure on strain localization in a 7050 aluminum alloy: Comparison of experiments and modeling for various textures, *Materials Science and Engineering: A* **661**, 187 – 197.

RUGGLES, T., CLUFF, S., MILES, M., FULLWOOD, D., DANIELS, C., AVILA, A. & CHEN, M. (2016a). Ductility of advanced high-strength steel in the presence of a sheared edge, *JOM* **68**, 1839–1849.

RUGGLES, T., FULLWOOD, D. & KYSAR, J. (2016b). Resolving geometrically necessary dislocation density onto individual dislocation types using EBSD-based continuum dislocation microscopy, *International Journal of Plasticity* **76**, 231 – 243.

WILKINSON, A.J. & BRITTON, T.B. (2012). Strains, planes, and EBSD in materials science, *Materials Today* **15**, 366 – 376.

WILKINSON, A.J., MEADEN, G. & DINGLEY, D.J. (2006). High resolution mapping of strains and rotations using electron back scatter diffraction, *Materials Science and Technology* **22**, 1–11.

YAN, D., TASAN, C.C. & RAABE, D. (2015). High resolution *in situ* mapping of microstrain and microstructure evolution reveals damage resistance criteria in dual phase steels, *Acta Materialia* **96**, 399 – 409.

ZHANG, T., COLLINS, D.M., DUNNE, F.P. & SHOLLOCK, B.A. (2014). Crystal plasticity and high-resolution electron backscatter diffraction analysis of full-field polycrystal Ni superalloy strains and rotations under thermal loading, *Acta Materialia* **80**, 25 – 38.